PHYSICAL REVIEW B VOLUME 37, NUMBER 7 1 MARCH 1988

Observed microscopic structure in the simulation of multilayers

Christopher D. Hruska* and James M. Phillips
Department of Physics, University of Missouri–Kansas City, Kansas City, Missouri 64110
(Received 26 October 1987)

A multilayer film was simulated by number, volume, and temperature ensembles. Systems of 224 and 672 molecules were scaled to methane and argon-graphite parameters. Studies were done at $T=25$ K for the coverages of 0.90 to 4.13 $(\sqrt{3}\times\sqrt{3})$ monolayers. The layers within the film are incommensurate in the methane but commensurate for the argon case. For methane, the first two layers are mutually modulated by rotated misfit dislocations.

The microscopic details of the intermolecular mechanisms in physical systems are, collectively, the genesis of the properties observed in thermodynamic experiments. Some of these details are often absent from analytic theories. Consequently, computer simulation and the accompanying graphic representation of finite sections of these systems can provide unique insights into the presence of the driving microstructures. The extent to which these microscopic mechanisms determine the properties of multilayers is then tested by the results of experiments using probes with the appropriate resolution. Our study concentrates on the first few layers of a film since it is reasonable to expect the interaction of these layers with the substrate will set the character of the multilayer growth.

Multilayer-growth criteria have been formally written in terms of the macroscopic thermodynamics of equilibrium by Bruch.[1] These conditions for monolayer (bilayer) to bilayer (trilayer) coexistence were applied to several different systems by Bruch and co-workers[2] and Phillips[3] in structurally "ideal" models. Other formulations have been given for elastic continuum models.[4,5] Lattice-gas models for epitaxy and growth behaviors in thick films have been studied.[6,7] Thermodynamic models have been reviewed.[8]

Computer simulations of the physiorption process with grand ensembles have been published.[9] We monitor the microstructure within an existing solid multilayer film similar to Vernov and Steele[10] rather than an attempt to observe the condensation of the three-dimensional 3D vapor into islands of adsorbate.

Our simulations are the logical continuation of a series of computational studies[3] for the methane on graphite system. The previous methods employed were lattice sums, lattice dynamics, and the quantum-mechanical cell model. The interaction potentials[3] have been well defined and a number of the results obtained by their use are quite close to experimental observation.[11] Some of the properties showing reasonable agreement include, a prediction of the registered $(\sqrt{3}\times\sqrt{3})$ monolayer, heats of adsorption for the monolayer and the bilayer, the transition temperature for the commensurate-incommensurate structural shift, and the overcompression of the near-neighbor distance in the bilayer to a value less than in bulk methane.[12]

With exactly the same interaction potentials our computer simulations should test some aspects of the structural assumptions made in all of the theoretical studies mentioned above.

The methane-methane and the methane-graphite interactions are based on atom-atom pair potentials with the parameters given by Severin and Tildesley.[13] At $T\geq 25$ K, the molecules may be in rotational diffusion,[14] so we have assumed a spherically symmetric methane molecule with a (12,6) LJ potential ($\epsilon/k=137$ K and $\sigma=3.6814$ Å). The methane graphite is given by Steele[15]

$$u(z)=\epsilon_{ls}\sum_{j=0}\left[\frac{2}{3}\left(\frac{\sigma_{\text{g.s.}}}{z+jd}\right)^{10}-\left(\frac{\sigma_{\text{g.s.}}}{z+jd}\right)^{4}\right],$$

with $\epsilon_{ls}/k=1468.5$ K, $\sigma_{\text{g.s.}}=3.297$ Å, and $d=3.37$ Å.

We have not included the MacLachlan substrate-mediated interaction and, of course, the zero-point contribution in the classical simulation. The overall effect is our scaling of methane will be slightly smaller than real methane. We accordingly report coverages in two ways: first as a density of molecules per unit area of the substrate, and second, for more realistic comparisons to laboratory coverages in units of $(\sqrt{3}\times\sqrt{3})$ monolayers. For the latter purpose, we define the uncompressed monolayer (zero spreading pressure) as the $(\sqrt{3}\times\sqrt{3})$ coverage of one. In any event, our coverages will be slightly higher than comparable conditions in a real experiment.

The argon on graphite system is approximated[1] in a similar way with

$$\epsilon/k=143.2\text{ K},\quad \sigma=3.35\text{ Å},\quad \epsilon_{ls}/k=995.4\text{ K},$$

$$\sigma_{\text{g.s.}}=3.1243\text{ Å},\quad d=3.20\text{ Å}.$$

It was pointed out by Krim[8] that the ratio of C_3 of the adsorption potential to the bulk cohesive energy is approximately 20% greater for the methane on graphite than for the argon on graphite system. This difference appears to be the key to the contrasting results we observe in the structural relationship of the first two layers of these systems.

During the simulations we calculate the ensemble averages for the internal energy, the integrated planar component of the pressure tensor, the 2D pair-distribution function (PDF) for each individual layer, and the probability distribution of molecules with height z above the substrate. Starting with an uncompressed monolayer with a density of 0.06 molecules/Å (Ref. 2) [coverage

$X=0.90(\sqrt{3}\times\sqrt{3})$ monolayers], we run 21 different coverages in an NVT ensemble for 224 and 672 molecules with periodic boundary conditions. The highest coverage was 4.13. Proceeding stepwise on the 25-K isotherm, each higher coverage used the rescaled positions of the final configuration of the previous simulation as the initial configuration of the next run. This method allows for shorter equilibration times and minimizes the shock of starting up a severely compressed ideal film. The runs are quite long (40000 to 80000 MC moves per molecule) and repeatable using slightly different starting conditions. In addition, we do extensive graphics views of the film at regular intervals during the simulation. The point of view is varied to five different positions for each layer and the entire film allowing a clear inspection for defects in any layer. We can superimpose one layer on an adjacent one for comparison. From this mass of information, we have been able to identify a number of interesting relationships in the microscopic structure of these films.

We believe the two most important features of our simulations are first, the contrast between the argon-graphite and the methane-graphite systems (see Figs. 1 and 2), and second, the mutually modulated structure (rotated misfit dislocations) occurring in the first two layers of the methane/graphite system (see Figs. 3 and 4). The low-temperature multilayer growth experiments on the argon-graphite system[16] indicate a uniform layer-by-layer growth (complete wetting) which is consistent with the quantitative results of Bruch and Wei.[2] It seems more than coincidence that our simulations (Fig. 2) show the first two argon layers to be within 0.2% of registry. This result agrees with, but well below, the experimental limits of the low-energy electron diffraction LEED measurements of Ref. 17 on the commensurability of the argon bilayer. Results for the configurations shown in Fig. 2 indicate two additional partial layers, with nearly bulk lattice constants, exist above the two lower complete layers.

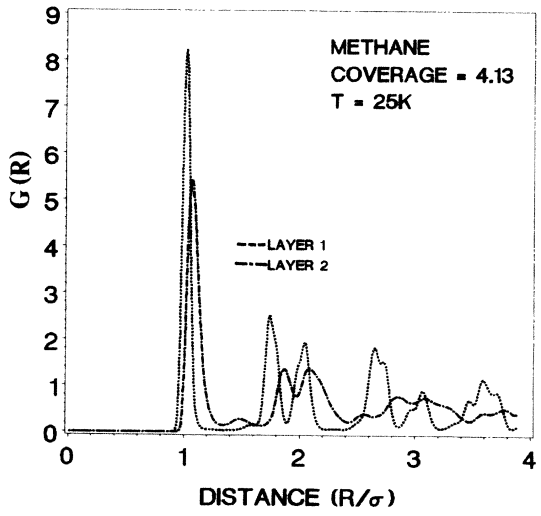

FIG. 1. A plot of the 2D pair distribution functions for the two layers of a trilayer of methane and graphite. The short-dashed curve is the first-layer curve and the dash-dotted curve is for the second.

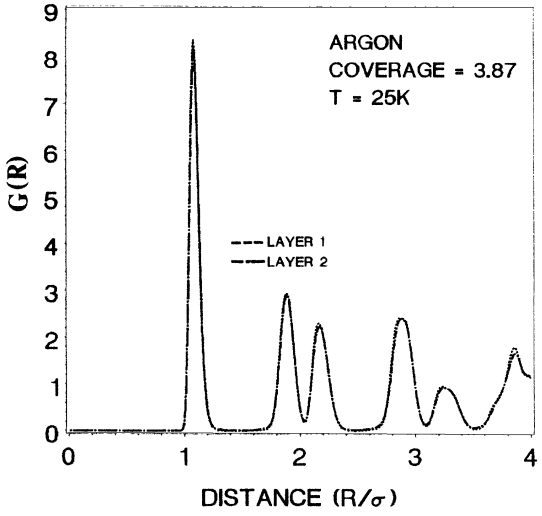

FIG. 2. A plot of the 2D pair-distribution function for the two layers of argon and graphite. The labels are the same as Fig. 1. The PDF's for these commensurate layers are superimposed.

Methane-graphite experiments[11,12,18] indicate complete wetting occurs only above the triple-point temperature. Recent neutron-diffraction results [12] suggest a better fit to the line shape is possible by assuming the first and second layers to be incommensurate. The fact that the same procedure for 672 molecules has the ability to form both commensurate and incommensurate phases for the argon and the methane systems (Figs. 1 and 2), respectively, illustrates the capability of the simulation to establish the registry of layers correctly. The area density ($\sim$0.27 molecules/Å^2) is nearly equal for the simulations shown in Figs. 1 and 2. The PDF for methane-graphite system shows the misfit between the first and second layers to be in the range of 2% to 5% over the range of our coverages. The commensurability observed in the argon case differs markedly from the misfit found at any methane coverage. The ensemble averages for all of the 21 coverages studied pass the usual equilibration criteria[19] and are in good agreement with the earlier calculated results.[3] A more complete comparison with theory will be reported elsewhere.

Shiba[20] predicts a rotated hexagonal structure for an elastic adlayer over a rigid periodic substrate (graphite). We observe a similar but fundamentally different interlayer response to incommensurability. The elastic constants of the methane layers are different only in that they are not equally compressed. This allows them to be mutually modulated in an interesting new pattern. The resulting structures are two oblique triangular lattices (Fig. 3)

$$|\mathbf{b}_1| < |\mathbf{a}_1| = |\mathbf{a}_2| < |\mathbf{b}_2|$$

with lattice vectors $(\mathbf{a}_1,\mathbf{b}_1)$ in the first (lowest) layer and $(\mathbf{a}_2,\mathbf{b}_2)$ for the second layer. The structure is uniaxial commensurate for rows parallel to the (**b**-**a**) direction, rotated for rows parallel to the **b** direction, and domain walled for rows parallel to the **a** direction. Figure 4 shows

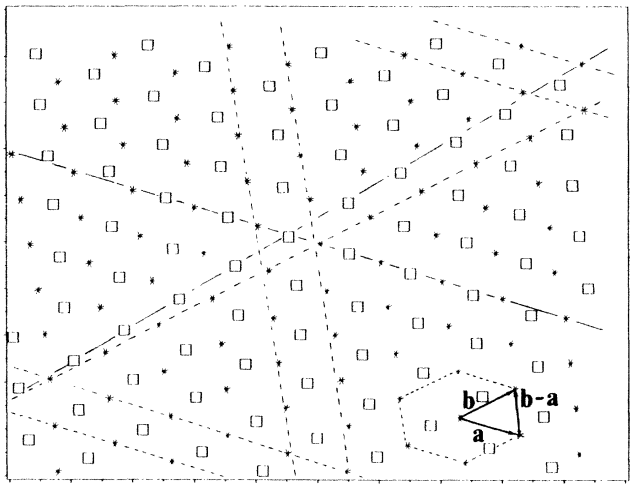

FIG. 3. A diagram of the final configuration of a bilayer of methane/graphite. The coverage is $X=2.84(\sqrt{3}\times\sqrt{3})$ monolayers and $T=25$ K. The stars mark the first-layer molecule positions and the squares the second layer.

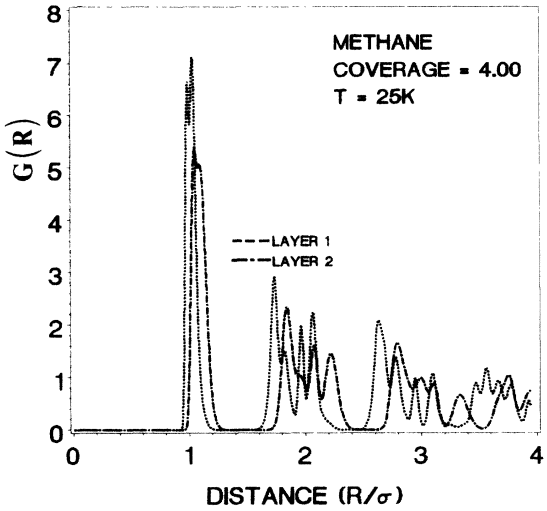

FIG. 4. A plot of the 2D pair-distribution functions of the first two layers in a trilayer of methane and graphite. The mutual modulation of the two layers is shown by the peak splitting.

the mutual modulation of the 2D PDF for each layer. Generally, the splitting of the peaks in the PDF is more defined in the highly compressed first layer. Thermal fluctuations tend to weaken the effects in the less compact second layer. This structure occurs in narrow ranges of coverage near bilayer and trilayer completion. There are few if any vacancies, slip planes, or edge dislocations within the first and second layers at these coverages. However, as the coverage is increased from the bilayer toward the trilayer coverages and as the coverage is pushed beyond the completed trilayer, defects are observed in the second layer. The presence of the defects destroys the mutual modulation and the peaks of the PDF are no longer split.

The finite-size section of our simulation must be viewed as a small part of a large domain-walled structure. This is because the uniaxial compression of both layers in the direction of the **a** vectors (Fig. 3) could not be sustained indefinitely. Eventually a wall intersection (hexagonal domains) or a kink (uniaxial domains) must relieve the increasing elastic strain with increasing sample size. Our simulations have emphasized the microstructure in multilayer systems and should in no way be considered of sufficient size or ensemble type to address the questions of the phase, separation, or width of domain walls. The new structure is repeatable since it has occurred at different coverages for both the bilayer and trilayer films. The simulation results in both clockwise and counterclockwise rotations. The commensurate rows and those parallel to a domain wall exchange directions for different runs. This flexibility demonstrates the sensitivity of the simulation to the subtleties of modulated structures. A quantitative difference can be seen in the rotation angle with the size of the sample. We estimate the angle by a Novaco-McTague model for the bilayer case (2°). The smaller system (224) has an angle of 4.1°. As the system is enlarged, the angle stablizes at 2.5°.

The microstructural observations of our simulations have suggested that interlayer commensurability and mutual modulation between layers may play a roll in multilayer growth and epitaxy.

We wish to thank L. Bruch, M. B. Webb, H. Taub, J. Larese, J. G. Dash, and S. C. Fain, Jr. for very helpful discussions. We thank the University of Missouri, Kansas City, Computer Science Program for the use of their parallel Elxsi Computer. Acknowledgment is made to the Donors of the Petroleum Research Fund, administered by the American Chemical Society, for the support of this research. C. D. H. thanks AT&T Technologies for their support.

*Present address: AT&T Technologies, Lee's Summit, MO 64063.

[1]L. W. Bruch and M. S. Wei, Surf. Sci. **100**, 481 (1980); M. S. Wei and L. W. Bruch, J. Chem. Phys. **75**, 4130 (1981).

[2]L. W. Bruch, J. M. Phillips, and X. -Z. Ni, Surf. Sci. **136**, 361 (1984); L. W. Bruch and X. -Z. Ni, Trans. Faraday Soc. Discuss. No. 80, (1985).

[3]James M. Phillips, Phys. Rev. B **34**, 2823 (1986); **29**, 4821 (1984); **29**, 5865 (1984); James M. Phillips and M. D. Hammerbacher, *ibid.* **29**, 5859 (1984); K. A. Hunzicker and James M. Phillips, *ibid.* **34**, 8843 (1986).

[4]D. A. Huse, Phys. Rev. B **29**, 6985 (1984).

[5]F. T. Gittes and M. Schick, Phys. Rev. B **30**, 209 (1984).

[6]C. Ebner, C. Rottman, and M. Wortis, Phys. Rev. B **28**, 4186 (1983).

[7]M. P. Nightingale, W. F. Saam, and M. Schick, Phys. Rev. B

30, 3830 (1984).

[8]Jacqueline Krim, Ph.D. thesis, University of Washington, 1984 (unpublished); J. G. Dash, Phys. Today **38**, 26 (1985); M. Bienfait, Surf. Sci. **162**, 411 (1985); R. J. Muirhead, J. G. Dash, and J. Krim, Phys. Rev. B **29**, 5074 (1984).

[9]D. Nicholson and N. G. Parsonage, *Computer Simulation and the Statistical Mechanics of Adsorption* (Academic, London, 1982); J. E. Lane and T. Spurling, Aust. J. Chem **29**, 2103 (1976).

[10]A. V. Vernov and W. A. Steele, Surf. Sci. **171**, 83 (1986).

[11]J. M. Gay, A. Dutheil, J. Krim, and J. Suzanne, Surf. Sci. **177**, 25 (1986); J. Krim, J. M. Gay, J. Suzanne, and E. Lerner, J. Phys. (Paris) **47**, 1757 (1986).

[12]J. Z. Larese, M. Harada, L. Passell, J. Krim, and S. Satija, Phys. Rev. B (to be published).

[13]E. S. Severin and D. J. Tildesley, Mol. Phys. **41**, 1401 (1980).

[14]D. R. Aadsen, Ph.D. thesis, University of Illinois, 1975 (unpublished); D. R. Baer, B. A. Fraass, D. H. Riehl, and R. O. Simmons, J. Chem. Phys. **68**, 1411 (1978).

[15]W. A. Steele, J. Phys. Chem. **82**, 617 (1978).

[16]J. L Seguin, J. Suzanne, M. Bienfait, J. G. Dash, and J. A. Venables, Phys. Rev. Lett. **51**, 122 (1983).

[17]C. G. Shaw, Ph.D. thesis, University of Washington, 1979 (unpublished); J. Unguris, L. W. Bruch, E. R. Moog, and M. B. Webb, Surf. Sci. **109**, 522 (1981).

[18]D. L. Goodstein, J. J. Hamilton, M. J. Lysek, and G. Vidali, Surf. Sci. **148**, 187 (1984); J. J. Hamilton and D. L. Goodstein, Phys. Rev. B **28**, 3838 (1983).

[19]H. Gould and J. Tobochnik, *An Introduction to Computer Simulation Methods* (Addison-Wesley, New York, 1987).

[20]H. Shiba, J. Phys. Soc. Jpn **46**, 1852 (1979); **48**, 211 (1980).